The RRM Domain of MINT, a Novel Msx2 Binding Protein, Recognizes and Regulates the Rat Osteocalcin Promoter†

Elizabeth P. Newberry, Tammy Latifi, and Dwight A. Towler*

Departments of Medicine and Molecular Biology and Pharmacology, Center for Cardiovascular Research, Division of Endocrinology, Diabetes, and Metabolism, Washington University School of Medicine, St. Louis, Missouri 63110

Received April 28, 1999; Revised Manuscript Received June 8, 1999

ABSTRACT: Msx2 is a homeodomain transcriptional repressor that exerts tissue-specific actions during craniofacial skeletal and neural development. To identify coregulatory molecules that participate in transcriptional repression by Msx2, we applied a Farwestern expression cloning strategy to identify transcripts encoding proteins that bind Msx2. A λgt11 expression library from mouse brain was screened with radiolabeled GST-Msx2 fusion protein encompassing the core suppressor domain of Msx2. A cDNA was isolated that encodes a novel protein fragment that binds radiolabeled Msx2. Homeoprotein binding activity was confirmed by Farwestern analysis of the T7-epitope-tagged recombinant protein fragment, and interactions in vitro require Msx2 residues necessary for transcriptional suppression in vivo. On the basis of biochemical analyses, this novel protein was named MINT, an acronym for Msx2-interacting nuclear target protein. The original clone is part of a 12.6 kb transcript expressed at high levels in testis and at lower levels in calvarial osteoblasts and brain. Multiple clones isolated from a mouse testis library were sequenced to construct a MINT cDNA contig of 11 kb. Starting from an initiator Met in good Kozak context, a large nascent polypeptide of 3576 amino acids is predicted, in contiguous open reading frame with the Msx2 interaction domain residues 2070−2394. Protein sequence analysis reveals that MINT has three N-terminal RNA recognition motifs (RRMs) and four nuclear localization signals. Western blot analysis of fractionated cell extracts reveals that mature ∼110 kDa (N-terminal) and ∼250 kDa (C-terminal) MINT protein fragments accumulate in chromatin and nuclear matrix fractions, cosegregating with Msx2 and topoisomerase II. In gel shift assays, the MINT RRM domain selectively binds T- and G-rich DNA sequences; this includes a large G/T-rich inverted repeat element present in the proximal rat osteocalcin (OC) promoter, overlapping three cognates that support OC expression in osteoblasts. MINT and OC mRNAs are reciprocally regulated during differentiation of MC3T3E1 calvarial osteoblasts. Consistent with its proposed role as a nuclear transcriptional factor, transient expression of MINT-(1−812) suppresses the FGF/forskolin-activated OC promoter, does not significantly regulate CMV promoter activity, but markedly upregulates the HSV thymidine kinase promoter in MC3T3E1 cells. In toto, these data indicate that the novel nuclear protein MINT binds the homeoprotein Msx2 and coregulates OC during craniofacial development. Msx2 and MINT both target an information-dense, osteoblast-specific regulatory region of the OC proximal promoter, nucleotides −141 to −111. The N-terminal MINT RRM domain represents an authentic dsDNA binding module for this novel vertebrate nuclear matrix protein. Acting as a scaffold protein, MINT potentially exerts both positive and negative regulatory actions by organizing transcriptional complexes in the nuclear matrix.

Osteoblast gene expression is an integrated response to the morphogenetic, mechanical, and metabolic demands placed upon skeletal tissues in vivo (*1*). During normal prenatal growth, endogenous developmental programs induced by regional morphogenetic cues largely determine the temporospatial patterns of osteoblast differentiation and tissue mineralization (*1*−*3*). Recently, a transcriptional hierarchy has emerged that controls ossification in the developing skull. The runt domain transcription factor, Cbfa1/Osf2,[1] provides the global competency to express the osteoblast phenotype throughout the entire skeleton, including the skull (*4*−*7*). Cbfa1/Osf2 recognizes cognates present in the promoters of osteocalcin (OC) (*4*, *5*, *8*), osteopontin (OPN) (*5*, *9*), and collagenase-3 (*10*), activating the expression of these genes in committed osteoprogenitors. By contrast, the homeodomain factors Msx1 and Msx2 control osteoblast differentiation and tissue mineralization in osseous tissues that arise from neural crest, heralding the regional influences of BMPs on craniofacial morphogenesis (*2*, *3*, *11*−*22*). Biochemically, Msx1 and Msx2 are transcriptional repressors that mediate suppression via protein−protein interactions with components of the basal osteoblast transcriptional machinery (*13*, *18*, *23*−*25*). Gene suppression by both Msx1 and Msx2 is independent of the intrinsic DNA binding

† This work was supported by NIH Grants AR43731 and DK52446 to D.A.T. and the Charles E. Culpeper Foundation. D.A.T. is a Charles E. Culpeper Medical Science Scholar.

* Address correspondence to this author at the Department of Bone Biology and Osteoporosis Research, Merck Research Laboratories, WP26A-1000, West Point, PA 19486. Phone: (215) 652-8273. Fax: (215) 652-4328.

10.1021/bi990967j CCC: $18.00
Published on Web 07/29/1999

activity of the Msx homeodomain (*13*, *24*). Dlx5—another homeodomain transcription factor expressed selectively in calvarial osteoblasts (*26*)—upregulates transcription of the osteoblast-specific osteocalcin gene by antagonizing Msx2-dependent transcriptional repression (*15*, *23*). Thus, while Cbfa1/Osf2 provides the mesenchymal cell with the global potential to express osteoblast genes such as osteocalcin and osteopontin, Msx and Dlx homeoproteins control the timing of stage-specific osteoblast gene transcription in the developing skull.

Although genetic and biochemical data support the general model of craniofacial skeletal gene transcription outlined above, careful analysis of Msx2, Msx1, and Cbfa1/Osf2 expression patterns during development indicates that additional levels of transcriptional regulation must exist. For example, the Cbfa1/Osf2 gene is first expressed at E12.5 in the murine skeletal anlage—two full embryonic days prior to the elaboration of osteoblast phenotypic markers such as osteopontin and osteocalcin (*1*, *5*−*7*, *27*). However, transient expression of Cbfa1/Osf2 in fibroblasts in culture rapidly activates the expression of both osteopontin and osteocalcin genes via TGYGGT cognates present in the promoters of these osteoblast genes (*5*, *6*). Similarly, Msx2 represses transcription of osteocalcin in neural crest-derived craniofacial odontoblasts and osteoblasts but not in the mesodermally derived osteoblasts of long bone (*13*, *18*, *21*, *28*). On the basis of these observations, we surmised that stage and cell-type-specific transcriptional coregulatory molecules must exist for both osteoblast homeoproteins and Cbfa1/Osf2.

A cadre of large coregulatory multiprotein complexes that function in both transcriptional activation and repression has been recently identified (*29*−*31*). These coregulators act as adapters—directing interactions between transcription factors and the preinitiation complex—and as chromatin remodeling enzyme complexes (*11*, *32*, *33*). We wished to identify whether a known or novel coregulatory scaffold protein might participate in homeoprotein action during craniofacial development. Therefore, we applied the Farwestern interaction cloning stategy of Blanar and Rutter (*34*) to identify cDNAs encoding Msx2 binding proteins expressed in brain, a craniofacial tissue that expresses Msx2 and a large fraction of the murine genome. We screened a well-characterized, random hexamer-primed λgt11 phage expression library from whole mouse brain using ^{32}P-radiolabeled GST-Msx2(55−208), encompassing the core suppressor domain. We identified a clone that encodes a novel ~35 kDa protein fragment that specifically binds Msx2, dependent upon Msx2 core suppressor domain residues 132−148. This novel protein fragment also binds the related homeoprotein Dlx5. The homeoprotein binding domain is part of a large, 3576 amino acid nascent polypeptide encoded by a 12.6 kb transcript that is expressed at high levels in testis and lower levels in bone, brain, and spleen. On the basis of functional analyses, we named this novel protein MINT, an acronym for Msx2 interacting nuclear target. Protein sequence analysis using ProfileScan and Pfam (*35*) reveals that MINT has three N-terminal RNA recognition motifs (RRMs) and four nuclear localization signals. Western blot analyses using antibodies directed to different domains of MINT reveal that the protein is processed into an N-terminal 110 kDa RRM domain fragment and a C-terminal 250 kDa fragment encompassing the original Msx2 binding domain. Analyses of the cytosolic, cytoskeleton, chromatin, and nuclear matrix fractions of MC3T3E1 osteoblasts reveal that both MINT protein fragments are greatly enriched in chromatin and nuclear matrix fractions, cosegregating with the nuclear markers. In gel shift assays with homopolymeric ssDNA, recombinant N-terminal MINT RRM domain binds avidly to poly(dG)-20 and dT-20, binds extremely poorly to poly(dU)-20, and does not bind poly(dA)-20 or poly(dC)-20. Consistent with its accumulation in the nuclear fraction of MC3T3E1 cells, MINT(1−546) also binds a dG/dT-rich imperfect inverted repeat element at nucleotides −141 to −111 in the rat OC proximal promoter, overlapping three well-described cognates that support OC expression in osteoblasts. Transient expression of MINT(1−812) has little effect on basal OC and CMV promoter (luciferase reporter) activities in osteoblasts but activates the basal HSV TK promoter 7-fold. However, MINT(1−812) selectively suppresses OC promoter activation by FGF2/FSK—stimuli that upregulate OC in part by promoting assembly of protein−DNA complexes on the OC promoter region recognized by MINT (1−546) in vitro. Taken together, these data indicate that the novel nuclear protein MINT binds the homeoprotein Msx2 and coregulates OC during craniofacial development. Msx2 and MINT both target an information-dense, osteoblast-specific regulatory region of the OC proximal promoter. As recently described for other transcription factors (*36*−*38*), the N-terminal MINT RRM domain represents an authentic DNA binding module for this novel vertebrate nuclear matrix protein. Acting as a scaffold, MINT may act by organizing transcriptional complexes in the nuclear matrix (*39*, *40*), modulating transcription factor access to promoter regulatory elements.

EXPERIMENTAL PROCEDURES

Chemicals, Cell Culture Media, Synthetic Oligodeoxynucleotides, and Molecular Biology Reagents. All chemicals, salts, and buffers for cloning and biochemical analyses were obtained from either Fisher Scientific (St. Louis, MO) or Sigma (St. Louis, MO). All Corning brand cell culture plasticware was purchased from Fisher. Cell culture media and serum were obtained from Summit (Fort Collins, CO) or Life Technologies (Gaithersburg, MD). Custom synthetic oligodeoxynucleotides were purchased from Life Technolo-

[1] Abbreviations: BMP, bone morphogenetic protein; BSA, bovine serum albumin; CMV, cytomegalovirus; CSPD, disodium 3-(4-methoxyspiro[1,2-dioxetane-3,2′-(5′-chloro)-tricyclo[3.3.1^{3,7}]decan]-4-yl)-phenyl phosphate; EDTA, ethylenediaminetetraacetic acid; EGTA, ethylene glycol bis(β-aminoethyl ether)-*N*,*N*,*N*′,*N*′-tetraacetic acid; FGF2, basic FGF; FSK, forskolin; GAPD, glyceraldehyde phosphate dehydrogenase; GST, glutathione *S*-transferase; Hepes, 4-(2-hydroxyethyl)-1-piperazineethanesulfonic acid; GTIR, G/T-rich inverted repeat; HSV, herpes simplex virus; IPTG, isopropyl thiogalactoside; LUC, luciferase; MINT, Msx2-interacting nuclear target protein; MOPS, 3-(*N*-morpholino)propanesulfonic acid; NLS, nuclear localization signal; OC, osteocalcin; OCFRE, osteocalcin FGF response element; OCFREB, OCFRE binding protein; ORF, open reading frame; OSE2, osteoblast-specific element 2; Osf2/Cbfa1, osteoblast-specific factor 2/core binding factor A1; PBS, phosphate-buffered saline; PCR, polymerase chain reaction; PMSF, phenylmethanesulfonyl fluoride; PVDF, poly(vinylidene difluoride); RACE, rapid amplification of cDNA ends; RRM, RNA recognition motif; SDS−PAGE, sodium dodecyl sulfate−polyacrylamide gel electrophoresis; SSAP, histone H1β promoter stage-specific activator protein; TBP, TATA box binding protein; kb, kilobase(s); hTAFII, human TBP-associated RNA polymerase II transcription factor; TFIIF, RNA polymerase II-associated transcription factor F; TK, thymidine kinase; Topo II, topoisomerase II.

gies (Gaithersburg, MD). Cloning reagents were purchased from Oncor (Gaithersburg, MD), Clontech (Palo Alto, CA), and Amersham Pharmacia Biotech (Piscataway, NJ). Radionuclides [γ-^{32}P]ATP (for Farwestern and gel shift analyses) and [α-^{32}P]dCTP (for cDNA probes) were purchased from Amersham (Arlington Heights, IL). Routine molecular biology enzymes and buffers were obtained from Promega (Madison, WI). The high-fidelity, Klentaq-based Advantage PCR kit was purchased from Clontech (Palo Alto, CA). All clones, subclones, and PCR products were sequenced using the ABI Prism Dye Terminator Kit (Foster City, CA).

Expression Cloning of Msx2 Binding Proteins, cDNA Cloning, RACE, and Sequence Analysis. The construction and characterization GST-Msx2(55−208) in Blanar vector pGEX2T[128/129] (*34*) have been previously described (*13*, *15*). Recombinant radiolabeled [^{32}P]GST-Msx2(55−208) was prepared precisely as previously detailed using [γ-^{32}P]ATP and protein kinase A (*13*). A commercially available, random hexamer-primed mouse brain λgt11 cDNA library (Clontech catalog no. ML3000b, Lot 37163, Palo Alto, CA) was screened using the Farwestern blot interaction cloning strategy of Blanar and Rutter (*34*) with our modified hybridization buffer (25 mM Hepes, pH 7.9, 50 mM NaCl, 5 mM $MgCl_2$, 0.1% Triton X-100, 1 mM DTT, and 1% nonfat powdered milk). Additionally, the basic Blanar and Rutter protocol (*34*) was modified by washing hybridized filters under conditions of increased stringency, at 42 °C, and in our modified hybridization buffer supplemented with 250 mM KCl. Approximately 350 000 recombinant phage were screened in the primary screen. At the level of secondary screens, phage inserts from plaque-purified clones were amplified by PCR using high-fidelity Klentaq (*41*). Briefly, phage plugs were eluted overnight at 4 °C in 1 mL of 35 mM Tris-HCl, pH 7.5/100 mM NaCl/10 mM $MgSO_4$ with 20 μL of chloroform. Phage DNA was ejected from 5 μL of phage eluate by denaturing for 5 min at 95 °C. Insert DNA was amplified using the Advantage PCR system (Clontech, Palo Alto, CA), with cycling parameters of 94 °C × 15 s, 55 °C × 30 s, and 72 °C × 4 min for 30 cycles with a 94 °C × 1 min preamplification treatment to activate the Klentaq polymerase. The PCR subcloning amplimers anneal to β-galactosidase (upstream primer; 5′-GAC TCC TGG AGC CCG TCA G-3′) and the right phage arm (downstream primer; 5′-GAC ACC AGA CCA ACT GGT AAT G-3′) in the λgt11 cloning vector. Agarose gel-purified amplified insert cDNA was sequenced to determine the ORF contiguous with β-galactosidase, digested with *Eco*RI, and then subcloned into the *Eco*RI site of pET23a (Novagen, Madison, WI). After PCR was used to identify subclones with the correct ORF orientation, T7-epitope-tagged recombinant proteins were produced as described (vide infra). For cDNA cloning, radiolabeled random hexamer-primed probes of novel cDNA inserts were used to serially screen a commercially available mouse testes cDNA library (catalog no. ML1020a, Clontech, Palo Alto, CA), using techniques previously described (*18*, *42*). Subcloning from λgt10 was performed by high-fidelity PCR as above, but using left phage arm (5′-CTT TTG AGC AAG TTC AGC CTG GTT AAG-3′) and right phage arm (5′-GAG GTG GCT TAT GAG TAT TTC TTC CAG GGT A-3′) amplimers. 5′-RACE and 3′-RACE were carried out using Marathon-Ready testes and brain cDNA kits purchased from Clontech (Palo Alto, CA). Sequence analysis was performed using ProfileScan software accessible from the ISREC Bioinformatics home page (Swiss Institute for Experimental Cancer Research; URL, http://www.isrec.isb-sib.ch/index.html), Pfam Hidden Markov Models software accessible from the Washington University Genetics website (URL, http://pfam.wustl.edu/hmmsearch.shtml), and DNAMAN version 4.0 software for Windows 95 purchased from Lynnon BioSoft (Vandreuil, Quebec, Canada).

Expression of T7-Tagged Recombinant Proteins in Escherichia coli, Purification, and Fractionation by SDS−PAGE. All recombinant protein fragments containing the N-terminal T7 tag were expressed from the T7 promoter of the prokaryotic vector pET23a (Novagen, Madison, WI). T7 fusion proteins were expressed in *E. coli* BL21(DE3) grown in minimal M9 media by a 3 h induction of T7 polymerase with 0.1 mM IPTG per the manufacturer's instructions. Typically, cells from 25 mL of each induced bacterial culture were collected by centrifugation, the cell pellets individually resuspended in 0.7 mL of complete lysis buffer (50 mM sodium phosphate, pH 8; 300 mM NaCl; 1 mM PMSF; 1 μg/mL leupeptin, pepstatin, and soybean trypsin inhibitor; 50 μg/mL aprotinin; 1 mM benzamidine; 0.2 mM sodium vanadate), and bacteria disrupted by sonication with a Branson 350 cell disruptor (3 × 20 s bursts at 4 °C). Following centrifugation at 10 000 rpm × 15 min × 4 °C, T7-recombinant proteins were isolated from the cleared bacterial extract by immunoprecipitation with anti-T7 antibody (Novagen; 0.5 μL/60 μL of bacterial extract) and protein G agarose (20 μL/precipitation; Santa Cruz Biotech, San Diego, CA). After the precipitates were washed with 1 mL of wash buffer (20 mM Hepes, pH 7.9, 150 mM NaCl, 0.5 mM EDTA, 0.1% Triton-X100), T7-tagged proteins were eluted by heating for 5 min at 85 °C in 30 μL of 1× SDS−PAGE sample buffer. Proteins were fractionated on 10% SDS−PAGE gels, electrotransferred to a nitrocellulose membrane, and analyzed by Farwestern blot analysis as previously described (*13*). The probes [^{32}P]GST-Msx2(55−208), [^{32}P]GST, [^{32}P]GST-Msx2(55−208; Δ132−148), and [^{32}P]GST-Dlx5(46−203) have been previously described in detail (*13*, *15*). Expression of T7 proteins was verified by Western blot using alkaline phosphatase-conjugated anti-T7 epitope antibody (1:10 000 dilution; Novagen, Madison, WI) and chemiluminescent detection with CSPD (Tropix, Bedford, MA). Recombinant MINT(1−546), MINT(2070−2394), and full-length TBP were expressed from pET23a in BL21(DE3) precisely as previously described (*13*).

Cell Culture, RNA Isolation, and Northern Blot Analyses of MC3T3E1 Osteoblasts. MC3T3E1 mouse calvarial osteoblasts were cultured as described (*43*) in α-modified Eagle's media and 10% fetal calf serum with penicillin/streptomycin. A7r5 and BHK21 cells were obtained from the American Type Culture Collection (Gaithersburg, MD) and grown per ATCC recommendations as described (*44*). To study the time course of RNA accumulation during osteoblast differentiation, cells were plated (10 cm diameter dishes, 10^5 cells/ cm^2) and subsequently maintained in growth media (*43*) supplemented with 50 μg/mL ascorbic acid for 0, 4, 7, 12, and 21 days. Total RNA was isolated, and 20 μg aliquots were analyzed by Northern blot analysis (*18*) at each time point after electrotransfer to Hybond-N (Amersham,

Arlington Heights, IL). RNA was isolated precisely as described (*18*) but with assiduous avoidance of excessive shear force (gentle mixing, no vortexing). Total RNA from homogenized mouse testis was the kind gift of Dr. Rodney Newberry (Washington University, St. Louis, MO). Radiolabeled probes for GAPD and OC were generated from subcloned PCR products previously described (*18*, *45*). The initial radiolabeled probe for analysis of MINT mRNA accumulation was generated from the Msx2 binding cDNA; confirmatory probes were subsequently obtained from newly isolated MINT 5′- and 3′-coding regions. The mouse multitissue Northern blot (2 μg of poly(A^+) mRNA per tissue sample lane) was purchased from Clontech (Palo Alto, CA).

Generation of Affinity-Purified Polyclonal Antibodies and Western Blot Analyses. Small, Cys-initiated synthetic peptides corresponding to MINT protein residues 92−110 and 2182−2199 (Figure 3, blue residues) were coupled to keyhole limpet hemacyanin and rabbit anti-peptide polyclonal sera generated by Zymed Laboratories, Inc. (South San Francisco, CA). Purified GST, GST-MINT(1−247), or GST-MINT(2070−2394) recombinant proteins were prepared using techniques previously detailed (*13*) and covalently coupled to cyanogen bromide-activated Sepharose (*46*). All preimmune and immune sera were pre-sorbed with GST-Sepharose. Subsequently, 5 mL of rabbit anti-MINT peptide immune serum (diluted with 45 mL of 10 mM Tris-HCl, pH 7.5) was adsorbed to 0.2 mL of either GST-MINT(1−247)-Sepharose or GST-MINT(2070−2394)-Sepharose and washed with 25 volumes each of 10 mM Tris-HCl, pH 7.5, and 10 mM Tris-HCl, pH 7.5/500 mM NaCl. Anti-MINT antibody was sequentially eluted with 4 × 0.5 mL of 100 mM glycine, pH 2.5, and each eluate was neutralized with 50 μL of 1 M Tris-HCl, pH 8. Purified anti-MINT antibody fractions were first assessed in Western blot analyses using 1 μg aliquots of recombinant purified MINT protein expressed in *E. coli* as described above. Typically, 1:500 to 1:2000 dilutions of affinity-purified anti-MINT polyclonal antibodies were used in all Western blot analyses. Immune complexes were visualized using chemiluminescent detection with alkaline phosphatase-conjugated goat anti-rabbit antibody (1:5000 dilution) and CSPD (Tropix, Bedford, MA) as previously described (*13*).

Biochemical Fractionation of MC3T3E1 Cell Extracts. MC3T3E1 cells were plated on 15 cm diameter tissue culture dishes (10^5 cells/cm^2) and cultured for an additional 3−5 days with fresh media changes every other day. After cell cultures were rinsed twice with ice-cold PBS, cells were scraped into PBS and collected by centrifugation at 1600 rpm × 5 min. Subsequently, cells were extracted and fractionated into cytosolic (Cyto), cytoskeletal (Csk), chromatin (Chr), and nuclear matrix (NM) fractions following the protocol of Merriman et al. (*39*); however, this was slightly modified by resuspension of the final nuclear matrix fraction in 8 M urea, 20 mM MOPS, pH 6.8, 1 mM EGTA, 0.1 mM $MgCl_2$, and 143 mM 2-mercaptoethanol. Protein recovery in each fraction was determined by the bicinchoninic acid assay (Pierce, Rockford, IL) after contaminants were removed following the method of Peterson (*47*). Equivalent amounts of protein were fractionated by Tris−acetate NUPAGE 3%−8% gradient gels (Novex, San Diego, CA) and electrotransferred to either PVDF or nitrocellulose for Western blot and Farwestern blot analyses, respectively. Anti-tubulin antibody TU-01 was purchased from Zymed (South San Francisco, CA). Anti-topoisomerase II antibody was purchased from TopoGen (catalog no. 2011-1, Columbus, OH). Anti-Msx antibody was purchased from Babco (catalog no. PRB-256C, Richmond, CA). Typically, these antibodies were used at 1:500 to 1:2000 dilutions in Western blot analyses.

Oligo(dT) Affinity Chromatography. Crude nuclear extracts were prepared following the method of Dignam et al. (*48*). Oligo(dT)−cellulose and cellulose columns (Sigma, St. Louis, MO) were preblocked in binding buffer (50 mM Tris-HCl, pH 7.5, 0.1% Triton X-100, 50 mM NaCl, 1 mM $MgCl_2$, 0.5 mM EGTA), supplemented with 0.2 mg/mL acetylated BSA, 0.2 mg/mL unacetylated BSA, and 0.25 mg/mL yeast tRNA. Nuclear proteins were bound in batch mode to either oligo(dT)−cellulose (0.1 mL of resin) or cellulose in column binding buffer for 45 min at room temperature. Subsequently, material was transferred to a microspin column (Costar), and the resins were washed (flow-through, 0.2 mL) and sequentially eluted with 0.1 mL fractions of binding buffer supplemented with increasing concentrations of NaCl (0.2, 0.5, and 1 M). Aliquots of each eluted nuclear protein fraction were resolved by 3%−8% NUPAGE polyacrylamide gels following the manufacturer's instructions (Novex, San Diego, CA). After electrotransfer to nitrocellulose, the fractionated nuclear proteins were analyzed by Farwestern and Western blots as described above.

Assessment of MINT(1−546) DNA Binding Activity by Electrophoretic Mobility Gel Shift Assays. Recombinant MINT(1−546) was expressed in *E. coli* from the prokaryotic expression vector pET23a as described above, purified by nickel chelate chromatography (Qiagen, Chatsworth, CA), and dialyzed exhaustively against the crude nuclear extraction buffer D of Dignam (*48*). Synthetic oligodeoxynucleotides corresponding to homopolymeric eicosamers were 5′-radiolabled with [γ-^{32}P]ATP and T4 polynucleotide kinase as previously described (*19*). Aliquots (∼50 ng) of recombinant MINT(1−546) were assayed for formation of protein−DNA complexes by gel shift assay and autoradiography. Gel shift assays were carried out as previously detailed (*19*), except that 0.5 μg of yeast tRNA rather than poly(dI·dC) was used in each binding reaction to prevent nonspecific DNA−protein interaction. Typically, 0.1 pmol of radiolabeled probe was present in the standard 20 μL binding reaction. Cold competition assays using ssDNA were performed with synthetic homopolymeric eicosamers as indicated. Cold competition assays using duplex DNA (dsDNA) were performed with annealed synthetic oligodeoxynucleotides corresponding to the rat OC promoter region −142 to −110 (upper strand 5′-AGT CAC CAA CCA CAG CAT CCT TTG GGT TTG ACC-3′, lower strand 5′-GGT CAA ACC CAA AGG ATG CTG TGG TTG GTG ACT-3′) or the duplex human MMP1 promoter Ets protein DNA binding cognate (upper strand 5′-CCT CAA GAG GAT GTT ATA CC-3′; lower strand 5′-GGT ATA ACA TCC TCT TGA GG-3′) (*44*). The Genbank accession number for the rat OC promoter is J04500.

Cellular Transient Transfection Assays. The rat OC−promoter−luciferase reporter construct 0.2 kb OCLUC (also known as 222 OCLUC, nucleotides −222 to +32) has been previously described (*19*). CMVLUC and HSV TKLUC promoter−reporter constructs were the kind gifts of Dr. John

Lawrence (University of Virginia) and Dr. Shun-ichi Harada (Merck, West Point, PA), respectively. The CMV-MINT-(1−812) eukaryotic expression construct was generated by introducing 5′-*Kpn*I and 3′-*Bgl*II (with stop codon) restriction sites onto the cDNA fragment encoding MINT residues 1−812; this fragment was subsequently subcloned into the *Kpn*I/*Bam*HI sites of pcDNA3 (Invitrogen, Carlsbad, CA) downstream of the CMV promoter in good Kozak context. MC3T3E1 calvarial osteoblasts were plated in Costar six-well cluster dishes (35 mm diameter wells, 7×10^5 cells/well). Cells were transiently transfected the following day precisely as previously described (*13*). All transfections incorporate a promoter−LUC reporter construct (to monitor either OC, CMV, or TK transcriptional activity), a CMV-β-galactosidase construct (to control for transfection efficiency), and varying amounts of pcDNA3-MINT(1−812) expression construct as indicated. Empty pcDNA3 expression plasmid was added to maintain a constant amount of DNA in each precipitation and transfection. Two days following transfection, cultures were re-fed with fresh media containing either vehicle or 3 nM FGF2/10 μM forskolin (*45*) and analyzed the following day for luciferase and β-galactosidase activities as previously detailed (*13*). All results presented were observed in a minimum of two independent replicate experiments.

RESULTS

Expression Cloning of a cDNA Encoding a Novel Msx2 Binding Protein. As discussed above, genetic, developmental, and biochemical analyses of Msx2 action indicate that the biological activities of this homeoprotein during craniofacial morphogenesis are cell-type specific. Our structure−function studies (*13*−*15*) demonstrate that transcriptional repression by Msx2 occurs via protein−protein interactions mediated by the core suppressor domain of Msx2 (residues 55−208). We wished to identify coregulatory proteins that potentially participate in Msx2 action in the developing central nervous system and bone. Therefore, we applied the Farwestern interaction blotting technique of Blanar and Rutter (*34*) to identify cDNAs expressed in mouse CNS that encode protein domains that bind Msx2. A commercially available, random hexamer-primed λgt11 library of mouse brain cDNA was screened with radiolabeled recombinant [^{32}P]GST-Msx2(55−208) expressed from Blanar vector pGEX2T[128/129], as described in Experimental Procedures. After plaque purification at the level of secondary screens, cDNA inserts were subcloned into pET23a for expression of T7-tagged fusion proteins in *E. coli* BL21(DE3). After induction, T7-tagged proteins were affinity purified with anti-T7 agarose, resolved by SDS−PAGE, and analyzed by Western and Farwestern blots. Two clones were isolated that contained an identical 1 kb cDNA insert encoding a protein of ∼35 kDa that binds GST-Msx2(55−208) (Figure 1, lanes 1 and 3). When expressed in *E. coli* (Figure 1, lane 1) or by in vitro transcription−translation (not shown), this T7-tagged Pro-rich protein fragment migrates with an apparent molecular mass of 66 kDa. This protein is not bound by either GST or the variant GST-Msx2(55−208; Δ132−148) lacking core suppressor domain residues (Figure 1, lanes 5 and 7); however, it does bind Dlx5, a homeoprotein related to Msx2 that is also expressed in bone (Figure 1, lane 9). By contrast, although TBP is well expressed (Figure 1, lane 2), none of these proteins bound TBP in Farwestern blot assay (lanes 4, 6, 8, and 10), demonstrating the specificity of protein−protein interactions between this clone's protein fragment and Msx2 or Dlx5. Genbank database analysis using NCBI Blast software (*49*) revealed that this clone was completely novel but did encode a putative nuclear localization sequence (vide infra). Northern blot analyses of RNA isolated from multiple mouse tissues (Figure 2A) and MC3T3E1 osteoblasts (Figure 2B) indicate that the cloned cDNA insert is part of a much larger 12.6 kb transcript. This mRNA is expressed at very high levels in testis and lower levels in brain, spleen, lung, liver, and kidney; little expression of the 12.6 kb transcript is detected in cardiac and skeletal muscle (Figure 2A) or ovary (data not shown). In cultures of differentiating MC3T3E1 calvarial osteoblasts, this large message is readily detected and dynamically regulated; with time-dependent terminal differentiation of MC3T3E1 cells, this novel 12.6 transcript is downregulated, with concomitant upregulation of the osteoblast-specific OC gene (Figure 2B, lanes 1−5). Levels of expression in MC3T3E1 cells and NIH3T3 cells are approximately equivalent to those found in spleen (∼10% the level in testis; Figure 2 and data not shown). On the basis of the Msx2 binding activity and functional characterization of this clone's gene product (vide infra), we named the protein MINT, an acronym for Msx2 interacting nuclear target protein.

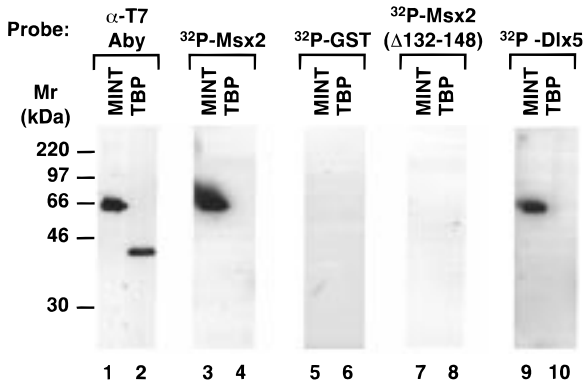

FIGURE 1: Msx2 interactions with a novel protein fragment depend on residues necessary for Msx2 core suppressor function. A λgt11 phage expression library from mouse brain was screened with radiolabeled Msx2 by the Farwestern interaction blotting technique. Inserts in contiguous ORF with β-galactosidase were subcloned into pET23a for expression of protein fragments as T7-epitope-tagged recombinants. Recombinant protein was analyzed by T7 Western blot (lanes 1 and 2) and Farwestern blot (lanes 3−10) as described in the text. Results are shown for one novel ORF identified that binds Msx2 (lanes 1, 3, 5, 7, and 9); recombinant T7-tagged TBP is shown as a negative control (lane 2, 4, 6, 8, and 10). On the basis of the functional characterization of this clone's gene product, we named the protein MINT, an acronym for Msx2 interacting nuclear target protein. The T7-tagged MINT fusion protein is predicted to be ca. 35 kDa but migrates at ca. 66 kDa on SDS−PAGE (lane 1), presumably due to its proline-rich sequence. Radiolabeled probes used for Farwestern blots were GST-Msx2-(55−208) for lanes 3−4, GST for lanes 5−6, GST-Msx2(55−208; Δ132−148) for lanes 7−8, and GST-Dlx5(46−203) for lanes 9−10. Note that Msx2 binds to the recombinant protein encoded by the novel MINT ORF (lane 3) but not to TBP (lane 4). GST does not bind either protein (lanes 5−6). Importantly, Msx2(Δ132−148)—lacking the 17 amino acid residues necessary for Msx2 core suppressor function in osteoblasts (*13*)—does not bind the novel MINT protein fragment (lane 7). Further note that the related osteoblast homeodomain protein, Dlx5, also binds MINT (lane 9) but not TBP (lane 10).

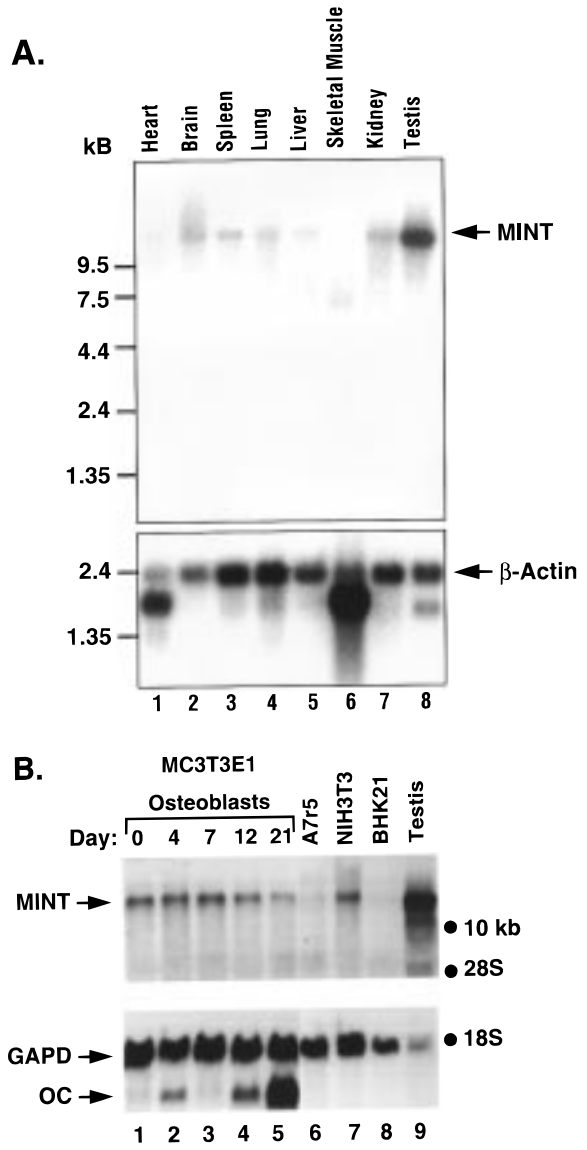

FIGURE 2: The novel MINT cDNA insert is part of a larger 12.6 kb transcript expressed in testis, calvarial osteoblasts, and other tissues. The initial ~1 kb cDNA inserts encoding the novel MINT protein fragment that was radiolabeled were used in Northern blot analyses of poly(A+) RNA isolated from multiple mouse tissues (panel A; 2 μg/lane) or total RNA isolated from differentiating MC3T3E1 calvarial osteoblast cultures and mouse testis (panel B; 20 μg/lane). Blots were probed with β-actin (panel A) or GAPD (panel B) as controls for RNA integrity. Differentiation was documented in cultures of MC3T3E1 cells by monitoring OC mRNA accumulation (panel B). Note that high levels of MINT transcript accumulate in testis (panel A, lane 8; panel B, lane 9). Lower mRNA levels accumulate in brain, spleen, lung, liver, and kidney (panel A, lanes 2−5 and 7); little if any expression of the 12.6 kb MINT transcript is detected in cardiac and skeletal muscle (panel A, lanes 1 and 6). Panel B: in cultures of differentiating MC3T3E1 calvarial osteoblasts, this large MINT transcript is also readily detected. MINT mRNA is downregulated as cultures differentiate, marked by the concomitant upregulation of OC expression (lanes 1−5). MINT mRNA expression in MC3T3E1 cells is approximately equivalent to that observed in spleen (~10% the level in testis). NIH3T3 fibroblasts also express MINT (lane 7); however, little if any MINT mRNA is detected in A7r5 vascular myoblasts (lane 6) or BHK21 cells (lane 8).

MINT cDNA Encodes a Pro- and Ser-Rich 391 kDa Basic Protein with RNA Recognition Motifs and Nuclear Localization Signals. Since levels of MINT expression were highest in testis, a testis λgt10 library was iteratively screened with radiolabeled cDNA inserts and overlapping clones sequenced to assemble an 10 841 base pair contig (Genbank accession number AF156529). The large MINT contig encodes a novel protein of 3576 residues in contiguous ORF (10 728 nucleotides) with an upstream Met codon in good Kozak consensus (*50*, *51*), the initial Msx2 binding domain, and a downstream stop codon (Figure 3). Reverse transcription PCR, 3′-RACE, 5′-RACE, and Northern blot analyses with multiple MINT cDNA probes confirmed that the same large message is expressed in MC3T3E1 murine calvarial osteoblasts and mouse testis (Figure 2 and data not shown). The 3576 amino acid nascent polypeptide product predicted (Figure 3) by translation of MINT mRNA is a 390 kDa basic protein (p*I* = 8.59), high in Pro (10.7%) and Ser (10.6% mol/mol) content. Overall, the N-terminal half of MINT is predicted to have a large helical content, while the C-terminal half of the protein is predicted to have extensive coil and β-strand content. The Msx2 binding domain MINT(2070−2394) is positioned at the transition point between the N-terminal helical and C-terminal Pro-rich domains. The predicted MINT protein sequence was analyzed by using Pfam (*35*, *52*) and ProfileScan software to identify established protein motifs. Two categories of motifs were unambiguously identified (Figure 3): three N-terminal RNA recognition motifs (RRM) and four nuclear localization signals (NLS). On the basis of these MINT protein primary sequence and domain analyses, we initiated directed functional characterization of MINT and its subdomains.

Mature MINT Accumulates as 110 kDa N-Terminal and 250 kDa C-Terminal Protein Fragments in Nuclear Chromatin and Nuclear Matrix Fractions. The presence of NLS motifs at residues 760−781, 984−1001, 1174−1191, and 2260−2277 strongly suggests that MINT is a nuclear protein. Moreover, since Msx2 acts a nuclear transcription factor, this additionally suggests a nuclear function for MINT. We wished to identify the size and subcellular localization of mature MINT protein in calvarial osteoblasts, a physiologically relevant background useful for studying Msx2 homeoprotein function. MC3T3E1 calvarial osteoblast cell extracts were biochemically fractionated into cytosolic, cytoskeleton, nuclear chromatin, and nuclear matrix components following a modification of the protocol of Fey and Penman (*35*, *39*, *53*). Tubulin (Tub) and topoisomerase II (Topo II) were used as markers of cytosolic and nuclear fractions, respectively. The distribution of MINT protein in these fractions was determined by Western blot analysis using affinity-purified anti-MINT polyclonal antibodies generated to N-terminal or C-terminal peptides as described in Experimental Procedures. As shown in Figure 4A (lower arrow), a 110 kDa protein immunoreactive with affinity-purified antibody directed to the MINT N-terminus is observed in nuclear chromatin (Chr) and nuclear matrix (NM) fractions, with a small amount also seen in the cytoskeletal (Csk) fraction. This pattern of MINT N-terminal protein accumulation closely mimics that of endogenous Msx immunoreactivity in MC3T3E1 cells (Figure 4A). An ~300 kDa protein is also detected in the cytoplasm with the MINT N-terminal antibody (Figure 4A, upper arrow) and potentially represents a nascent polypeptide precursor (vide infra). The efficiency of fractionation was confirmed with anti-tubulin antibody, which identified the ~50 kDa tubulin protein only

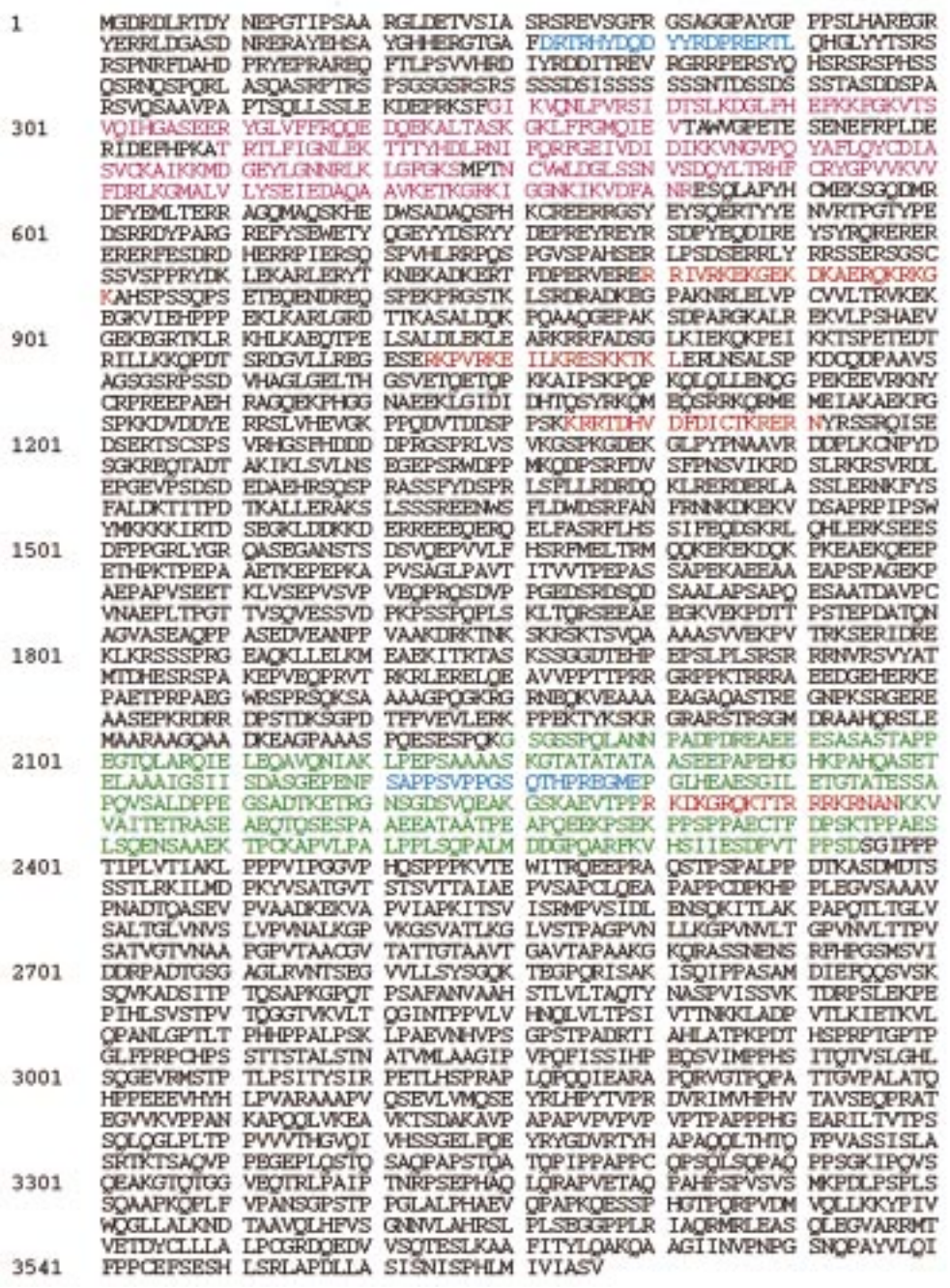

FIGURE 3: The MINT transcript predicts a nascent polypeptide of 3576 amino acids, encoding three N-terminal RNA recognition motifs and four nuclear localization signals. A testis λgt10 library was iteratively screened with radiolabeled MINT cDNA inserts and multiple overlapping clones sequenced to assemble a 10 838 base pair contig (Genbank accession number AF156529). The MINT contig encodes a novel protein of 3576 amino acids in contiguous ORF (10 728 nucleotides) with an upstream Met codon in good Kozak context, the initial Msx2 binding fragment, and a downstream stop codon. The three RRMs are outlined in pink, while the four NLS motifs are outlined in red. The initial Msx2 binding domain is in green, and the sequences used to generate the affinity-purified anti-peptide antibodies for studies presented in Figures 4 and 5 are in blue. Upon sequencing of multiple clones and RT-PCR products, apparent allelic polymorphisms were observed at the following residues: 823 (Met in lieu of Lys), 862 (Ala in lieu of Thr), 874 (Ser in lieu of Ala), 1043 (Ala in lieu of Val), 1591 (Val in lieu of Ile), 1637 (Ala in lieu of Val), 2479 (Ala in lieu of Val), 2506 (Val in lieu of Asp), 2942 (Pro in lieu of Leu), and 3465 (Val in lieu of Met).

in cytosolic and cytoskeletal fractions (Figure 4A). To confirm that the 110 kDa MINT protein encoded nucleic acid binding function as predicted by the RRM motifs (Figure 3 and vide infra), we studied the chromatographic character of this protein on commercially available oligo(dT)−cellulose, analyzing elution profiles by Western blot analysis. As shown in Figure 4B, the 110 kDa protein efficiently binds to oligo(dT)−cellulose [no MINT protein in the flow-through fraction (FT)] and elutes only with high NaCl concentrations. By contrast, the 110 kDa MINT fragment does not interact efficiently with cellulose resin lacking conjugated nucleic acid, largely appearing in flow-through (FT) and low NaCl elution fractions. Thus the N-terminal domain of MINT encompassing the RRM domains accumulates as a 110 kDa protein fragment in the nuclear fractions of MC3T3E1 calvarial osteoblasts.

Using an antibody raised against the C-terminal Msx2 binding domain MINT(2070−2394), a 250 kDa MINT

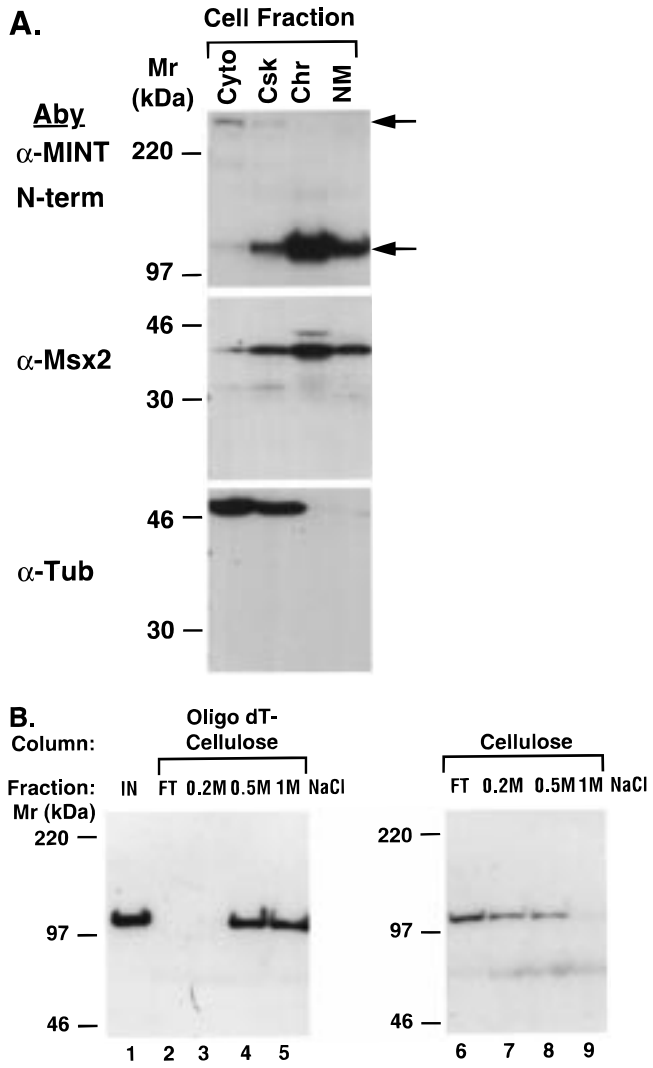

FIGURE 4: The mature MINT RRM domain accumulates as a 110 kDa N-terminal protein fragment in nuclear fractions of MC3T3E1 calvarial osteoblasts. Panel A: MC3T3E1 cell extracts were biochemically fractionated into cytosolic (Cyto), cytoskeletal (Csk), chromatin (Chr), and nuclear matrix (NM) components as detailed (*39*) and equivalent amounts of protein and analyzed by Western blot. Affinity-purified anti-MINT antibody directed against the MINT N-terminus (Figure 3) was used to localize the MINT N-terminal (RRM) domain. Anti-Msx antibody and anti-tubulin antibodies were utilized to evaluate the efficiency of nuclear (Msx2) and cytosolic (tubulin) fractionation. Note that a MINT protein fragment of 110 kDa is observed in nuclear chromatin and nuclear matrix fractions (lower arrow). Further note that only a very small amount of the MINT N-terminal protein is observed in the Csk fraction and closely mimics the pattern of Msx2 accumulation. In these same fractions, Tub immunoreactivity is observed only in Cyto and Csk fractions. An ~300 kDa cytoplasmic protein is faintly visible in the cytoplasmic fraction and may represent an incompletely processed precursor (upper arrow; see text). Panel B: chromatographic separation of crude nuclear extracts on oligo(dT)−cellulose (lanes 2−5) or cellulose without nucleic acid (lane 6−9), followed by SDS−PAGE and Western blot analysis using antibody recognizing the MINT N-terminal RRM domain. Oligo(dT) affinity chromatography of MC3T3E1 nuclear extracts reveals that the endogenous 110 kDa MINT fragment binds nucleic acid; note that MINT immunoreactive 110 kDa protein efficiently binds to oligo(dT)−cellulose [compare input, lane 1, with column flow-through (FT), lane 2] and elutes with high salt (lanes 4 and 5). MINT is found primarily in the flow-through fraction in the absence of nucleic acid coupling to cellulose (lane 6).

protein fragment is observed that accumulates only in the chromatin (Chr) and nuclear matrix (NM) fractions (Figure 5, lanes 1−4). This protein comigrates and cofractionates with a 250 kDa protein that specifically binds radiolabled GST-Msx2 by Farwestern blot (Figure 5, lanes 5−8); it does not bind radiolabeled GST (lanes 9−12). The efficiency of fractionation is again demonstrated, since the nuclear protein Topo II is identified primarily in the nuclear chromatin fraction (Figure 5, lanes 13−16). Thus, consistent with the presence of four NLS motifs, mature MINT proteins of 110 kDa (contains the N-terminal RRM domain) and 250 kDa (contains the initial Msx2 binding domain) accumulate in the nuclear fractions of MC3T3E1 osteoblasts. Given the protein predicted from the MINT cDNA contig, the nascent MINT polypeptide must be proteolytically processed. The ~300 kDa protein detectable in the cytoplasm with the N-terminal antibody (Figure 4A, upper arrow) potentially represents an incompletely processed precursor.

The N-Terminal RRM Domain MINT(1−546) Exhibits Sequence-Specific DNA Binding Activity. The identification of RRMs (*54*) at MINT residues 269−341, 370−446, and 450−522 strongly suggests that MINT possesses nucleic acid binding function. Moreover, the biochemical localization of MINT protein to nuclear matrix and chromatin fractions and interaction of MINT with homeodomain transcription factors suggested that MINT might also be a transcriptional regulator and bind DNA. Of note, a novel sea urchin transcription factor, SSAP, has been recently shown to regulate the histone H1β enhancer via two tandem RRMs that function as a ssDNA and dsDNA binding domain (*36*, *37*). Therefore, we directly assessed whether recombinant MINT(1−546)—encompassing the three RRMs between residues 269 and 522 (Figure 3)—exhibits DNA binding activity. Purified recombinant MINT(1−546) was first tested for ssDNA binding activity using radiolabeled homopolymeric eicosamers of dG, dA, dT, dC, and dU in gel shift assays. As shown in Figure 6A, MINT(1−546) binds avidly to dG-20 and dT-20; by contrast, MINT(1−546) does not bind dA-20, dC-20, or dU-20. The initial Msx2 binding domain MINT(2070−2392) does not exhibit DNA binding to any of these oligos (data not shown). Binding specificity was confirmed by competition assays, using radiolabeled dT-20 as a probe; as shown in Figure 6B, unlabeled dT-20 and dG-20 compete for binding of MINT(1−546) to radiolabeled dT-20, while unlabeled dU-20, dA-20, and dC-20 do not compete. Intriguingly, addition of unlabeled dG-20 also gives rise to a larger, "supershifted" DNA−protein complex (Figure 6B, lanes 14−16), suggesting multimerization. By contrast, dT-20 gives rise only to monotonic competition (Figure 6B, lanes 1−3), indicating overlapping yet distinct binding modalities for dG-20 and dT-20 to MINT. Thus, like SSAP, MINT exhibits sequence-specific DNA binding activity encoded in the N-terminal MINT RRM domain.

MINT(1−546) Binds a G/T-Rich Element in the Proximal Rat OC Promoter. On the basis of the T- and G-binding site selectivity of MINT observed in homopolymeric gel shift assays (Figure 6), we next examined whether any G/T-rich elements were present in the rat OC promoter, a target of Msx2 action in osteoblasts and odontoblasts. One region of interest was identified—a 31 bp, imperfect inverted repeat element (base pairs −141 to −111) composed of two G/T-rich motifs, each motif differentially positioned on lower and

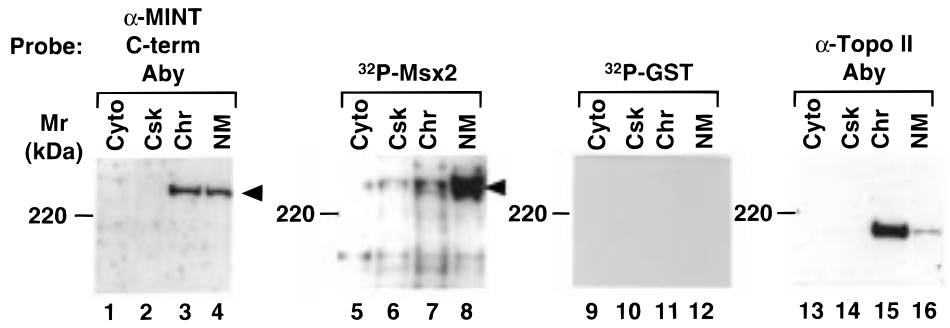

FIGURE 5: The mature MINT Msx2 binding domain accumulates as a 250 kDa protein fragment in nuclear fractions of MC3T3E1 calvarial osteoblasts. MC3T3E1 cell extracts were fractionated and proteins resolved for Western blot as outlined in the legend to Figure 4. Affinity-purified anti-MINT antibody directed against the MINT midmolecule (Figure 3) was used to localize the MINT Msx2 binding domain. Note that a MINT protein fragment of 250 kDa is observed in nuclear chromatin and nuclear matrix fractions (lanes 3 and 4, arrowhead) but not in cytosolic or cytoskeletal fractions (lanes 1 and 2). This protein precisely comigrates with a Msx2 binding protein revealed by Farwestern blot analysis using radiolabeled Msx2 (lanes 5−8, arrowhead). This interaction is specific, since radiolabeled GST does not bind this protein (lanes 9−12). Fractionation was monitored by assessing Topo II immunoreactivity, a marker for chromatin and nuclear matrix compartments (lanes 13−16). See text for details.

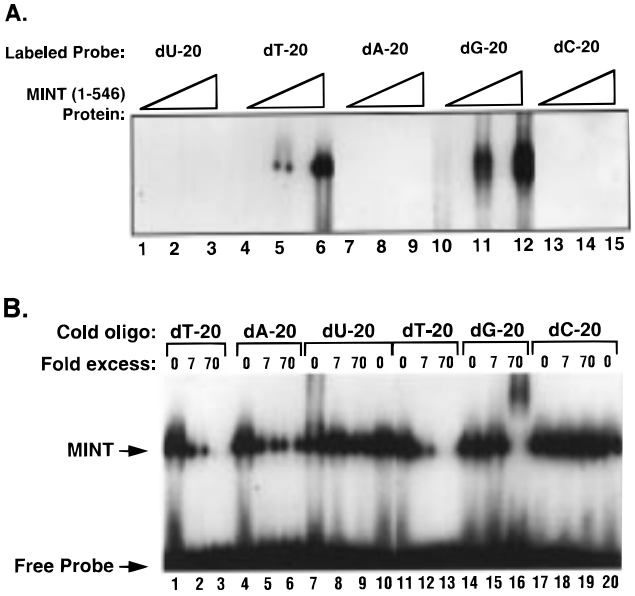

FIGURE 6: Recombinant MINT(1−546) that possesses the N-terminal RRM domain binds homopolymeric dG and dT single-stranded DNA. Panel A: recombinant purified MINT(1−546) protein was prepared and assessed for ssDNA binding activity using radiolabeled homopolymeric eicosamers dU-20, dT-20, dA-20, dG-20, and dC-20 by gel shift assay as outlined under Experimental Procedures. Lanes: 1, 4, 7, 10, and 13, no extract (10 μg of BSA only); 2, 5, 8, 11, and 14, gel shift observed using 100 ng of purified MINT(1−546) protein; 3, 6, 9, 12, and 15, gel shift observed using 200 ng of purified MINT(1−546) protein. Note that MINT(1−546) forms specific protein−DNA complexes with dT-20 (lanes 4−6) and dG-20 (lanes 10−12) but not with dU-20 (lanes 1−3), dA-20 (lanes 7−9), or dC-20 (lanes 13−15). The free radiolabeled probe is run off the bottom of these gels. Under identical conditions, recombinant purified MINT(2070−2394) does not form complexes with any of these oligos (not shown). Panel B: specificity of MINT-(1−546) protein−ssDNA interactions assessed by competition analyses. Gel shift assays were performed using radiolabeled dT-20 probe and recombinant MINT(1−546), in either the absence or presence of excess unlabeled "cold" eicosameric oligos. Note that unlabeled oligo(dT) (lanes 1−3) competes for MINT(1−546) binding to labeled dT-20. Further note that dA-20 (lanes 4−6) only weakly competes, while dU-20 (lanes 7−10) and dC-20 (lanes 17−20) do not compete at all. Finally, note that unlabeled dG-20 (lane 14−16) competes poorly but additionally gives rise to a "supershifted," slowly migrating complex (lane 16). This supershifted complex is not observed with unlabeled dT-20 competition (lanes 1−3), indicating distinct binding modalities of dT-20 and dG-20 to MINT.

FIGURE 7: The proximal rat OC promoter region −141 to −111 encodes a G/T-rich imperfect inverted repeat that overlaps three important osteoblast regulatory elements. The upper strand sequence of the rat OC promoter region −144 to −106 is shown. As depicted, this region encodes the OCFRE at −144 to −138 (*45*), the OSE2 element recognized by Cbfa1/Osf2 at −134 to −129 (*4*, *5*, *8*), and a steroid hormone element half-site that participates in cAMP induction at −114 to −109 (*43*). The center of the G/T-rich (C/A on left arm upper strand) imperfect inverted repeat is indicated by a filled circle, and the two arms of the repeat are indicated by arrows.

upper strands (Figure 7; numbering relative to the start site of OC transcription). We wished to directly test if MINT could bind this G/T-rich region of the proximal rat OC promoter and thus assessed whether recombinant MINT(1−546) recognizes proximal OC promoter fragments in gel shift assay. As shown in Figure 8, recombinant MINT(1−546) binds to the radiolabeled OC promoter region −142 to −110 corresponding to the G/T-rich inverted repeat (GTIR; lane 1). Importantly, binding is sequence specific; while the unlabeled homologous duplex oligo(OC GTIR) is capable of competing for MINT−OC promoter DNA interactions (Figure 8, lanes 2 and 3), a duplex sequence derived from the matrix metalloproteinase-1 proximal promoter, MMP1 ETS (*44*), cannot compete (Figure 8, lanes 4−6). By contrast, the single-stranded DNA dG-20 (Figure 8, lanes 7−9) competes for MINT binding to the OC promoter. dT-20 only very weakly competes (lanes 16−18), and dA-20 (lanes 10−12), dU-20 (lanes 13−15), and dC-20 (lanes19−20) do not compete at all. Thus, MINT(1−546) specifically binds to the G/T-rich OC promoter region −142 to −110, overlapping cognates that support basal (*19*) and FGF2/FSK-stimulated (*43*, *45*) OC promoter activity in osteoblasts.

We wished to confirm that MINT(1−546) is capable of recognizing dsDNA cognates in the OC promoter. PCR was utilized to generate a duplex DNA fragment of the OC promoter region −222 to −90, encompassing the imperfect inverted repeat at nucleotides −141 to −111. The 133 base pair, dsDNA OC promoter fragment was agarose gel-purified, 5′-labeled with T4 kinase and [γ-^{32}P]ATP, and utilized in gel shift assay as described in Experimental Procedures. As shown in Figure 9, while BSA does not bind

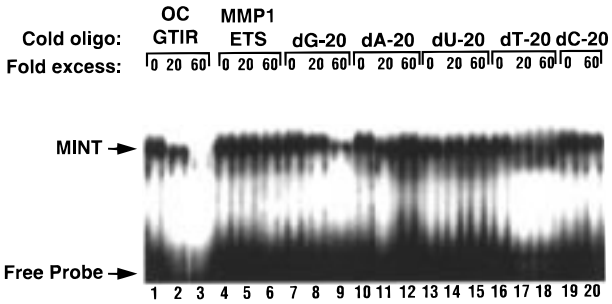

FIGURE 8: MINT(1−546) binds to the OC promoter region −142 to −110 in gel shift assay. Recombinant purified MINT(1−546) was prepared and assessed for double-stranded DNA binding activity using radiolabeled duplex OC promoter fragment −142 to −110 containing the imperfect inverted repeat (Figure 7). Note that MINT(1−546) binds to the OC promoter region −142 to −110 (lane 1). DNA binding is specific; while the unlabeled homologous synthetic duplex oligonucleotide competes for binding (lanes 2−3; OCGTIR), the Ets cognate found in the human MMP1 promoter does not compete (lanes 4−6). Further note that homopolymeric ssDNA was less efficient in competition; while single-stranded dG-20 (lanes 7−9) competes for MINT(1−546) binding to the OC promoter fragment, dA-20 (lanes 10−12), dU-20 (lanes 13−15), and dC-20 (lanes 19−20) do not compete. dT-20 (lanes 16−18) only very weakly competes for binding of MINT(1−546) to the OC GTIR duplex oligo.

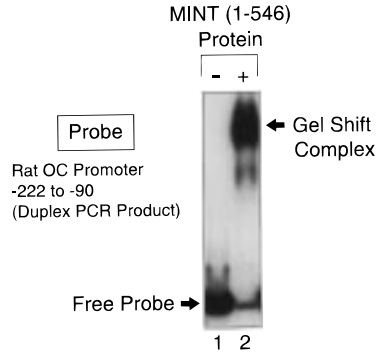

FIGURE 9: Recombinant MINT(1−546) binds the 133 base pair rat OC promoter fragment −222 to −90 in gel shift assay. PCR was used to generate the 133 base pair double-stranded DNA OC promoter fragment −222 to −90, encompassing the G/T-rich imperfect inverted repeat at −141 to −111. This PCR fragment was gel purified, 5′-radiolabeled, and assessed for recognition by recombinant MINT(1−546) in gel shift assay. Lanes: 1, no recombinant MINT protein (1000 ng of BSA only); 2, gel shift complex observed in the presence of 200 ng of recombinant MINT-(1−546). Note that MINT forms a gel shift complex with the 133 base pair OC promoter fragment (lane 2, arrow) and binds >90% of the radiolabeled probe, confirming the double-stranded DNA binding activity of MINT(1−546).

this 133 base pair OC promoter fragment (lane 1), 200 ng of recombinant purified MINT(1−546) forms a gel shift complex with the radiolabeled dsDNA PCR product (lane 2). Greater than 90% of the dsDNA probe present in this assay is bound by the recombinant MINT protein as indicated by the decrements and increments in the free probe and gel shift complex, respectively. Thus, MINT(1−546) binds the 133 base pair OC promoter PCR fragment −222 to −90 in gel shift assay, confirming the dsDNA binding activity of MINT.

MINT (1−812) Acts both as a Promoter-Selective Transcriptional Repressor and as an Activator in MC3T3E1 Calvarial Osteoblasts. We wished to assess the transcriptional consequences of MINT RRM domain binding to the proximal OC promoter. Therefore, we transiently expressed a MINT protein fragment encompassing the 90 kDa N-terminal MINT domain from the CMV promoter in MC3T3E1 osteoblasts and assessed effects on transcription directed by the proximal rat OC promoter (0.2 kb fragment), the human CMV promoter (0.3 kb fragment), and human HSV TK promoter (0.1 kb fragment). The firefly luciferase gene was used as the reporter for all three promoters. As shown in Figure 10A, pcDNA3-MINT(1−812) slightly decreases the basal transcriptional activity of 0.2 kb OCLUC by 15% and does not significantly promote activity of CMVLUC. Surprisingly, pcDNA3-MINT(1−812) markedly upregulates the activity of HSV TKLUC in MC3T3E1 calvarial osteoblasts. Since MINT(1−546) binds to the proximal OC promoter region activated by FGF/FSK (*45*), we assessed whether activation of the promoter via these elements influences the regulatory actions of pcDNA3-MINT(1−812) on OC. As shown in Figure 10B, while pcDNA3-MINT(1−812) has little effect on the basal OC promoter, it suppresses the FGF/FSK-activated OC promoter by ca. 50%. Thus, the N-terminal MINT RRM domain functions as a promoter-specific transcriptional regulator in calvarial osteoblasts; MINT(1−812) represses FGF/FSK activation of the proximal OC promoter, has no significant effect on the CMV promoter, but markedly upregulates transcription from the basal TK promoter.

DISCUSSION

The mechanisms whereby dispersed homeodomain transcription factors regulate gene expression are poorly understood. Traditionally, the homeobox-encoded homeodomain is characterized as a DNA binding domain that directs monomeric protein−DNA interactions at A/T-rich promoter cognates (*55*, *56*). However, accumulating evidence indicates that the N-terminal arm and extension of the homeodomain direct protein dimerization events necessary for homeoprotein function (*15*, *23*, *55*, *56*). In yeast, the prototypic homeodomain suppressor MATα2 acts in concert with the MADS box factor MCM1 to control mating phenotype. MATα2 suppressor function depends on dimerization with MCM1—directed by the homeodomain N-terminal extension—and DNA binding activity provided by the homeodomain (*57*). By contrast, transcriptional repressor function of the vertebrate homeoprotein Msx2 is independent of homeodomain DNA binding activity (*13*−*15*). Protein−protein interactions directed by the Msx2 homeodomain N-terminal arm and extension remain important for function (*13*−*15*). Msx2 binds TFIIF and suppresses basal transcription in part via this component of the preinitiation complex (*13*). However, Msx2 must require the DNA binding activity of other, coregulatory partners to provide promoter specificity for Msx2-dependent transcriptional repression (*14*, *15*, *23*, *55*).

We have mapped Msx2 responsiveness to the osteoblast-specific 0.2 kb OC promoter, base pairs −222 to +32 (*13*−*15*, *19*). Msx2 inhibits specific protein−DNA interactions at an element in the proximal OC promoter necessary for FGF-dependent transcriptional activation (OCFRE at bp −142 to −138) (*14*). By contrast, Msx2 has no effect on protein−DNA interactions at a second, more distal element necessary for transcriptional activation of OC expression by calcitriol (*14*). Intriguingly, the Msx2 binding protein, MINT, also recognizes this region of the OC promoter. There are

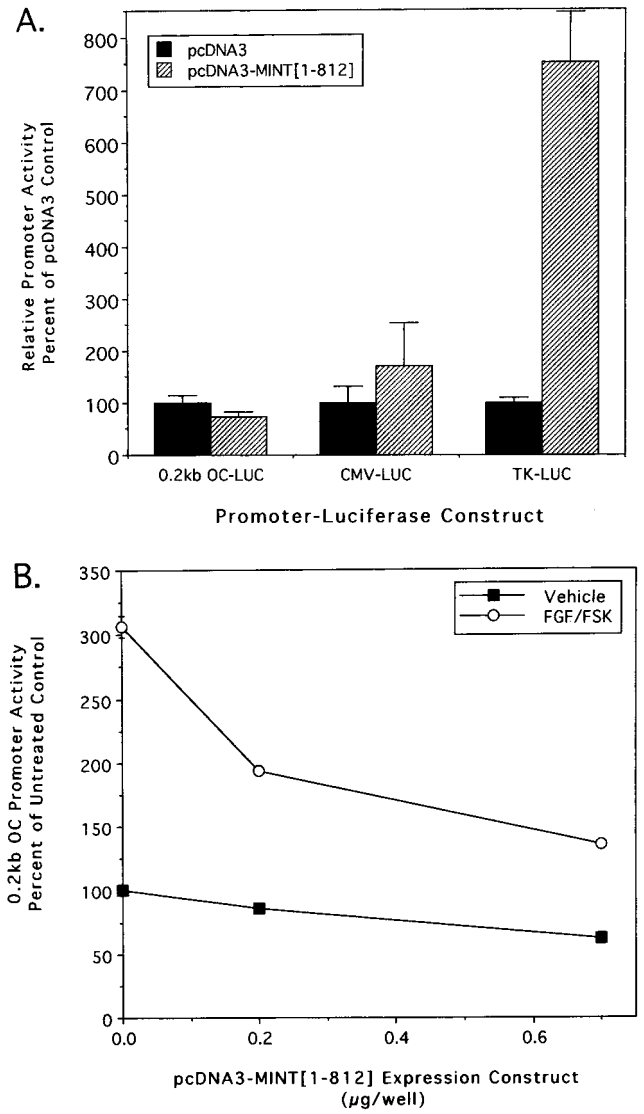

FIGURE 10: MINT(1−812) exhibits promoter-specific transcriptional regulation in MC3T3E1 mouse calvarial osteoblasts. MC3T3E1 calvarial osteoblast cell cultures were transfected with OC-LUC, CMV-LUC, and TK-LUC promoter−luciferase reporter constructs (1 μg/well) as detailed in Experimental Procedures, along with either pcDNA3 or pcDNA3-MINT(1−812) expression plasmid (400 ng/well) as indicated. CMV-β-galactosidase (700 ng/well) was included as an internal control for transfection efficiency, and empty pcDNA3 expression vector was used to maintain constant DNA concentrations in all transfections. Data presented are representative of results obtained in two to four independent experiments. Panel A: data are presented as the mean (±SD) luciferase activity observed in independent triplicate transfections, expressed as a percent of basal OC-LUC, CMV-LUC, or TK-LUC promoter activity observed in the absence of pcDNA3-MINT(1−812). Note that pcDNA3-MINT(1−812) has little if any effect on basal OC and CMV promoter activities but markedly upregulates TK promoter activity. Panel B: pcDNA3-MINT(1−812) suppression of FGF/FSK-activated OC promoter activity. Data are presented as the mean (±range; variation <2%) luciferase activity observed in independent duplicate transfections, expressed as a percent of the basal 0.2 kb OC-LUC activity observed in the absence of pcDNA3-MINT and FGF/FSK. Note that pcDNA3-MINT(1−812) preferentially suppresses the FGF2/FSK-activated OC promoter. See text for details.

several important and intriguing features of this element, 5′-GTCACCAACCACAGCA·TCCTTTGGGTTTGAC-3′ (upper strand sequence shown with arms of imperfect G/T-rich inverted repeat underlined, center indicated by filled circle; see Figure 7). First, as mentioned above, we previously identified that DNA−protein interactions in this region of the OC promoter are important targets of Msx2 action. Second, this element falls within the proximal OC promoter region that exhibits osteoblast specificity in vitro (*12*, *19*) and in vivo (*58*). Third, the element overlaps three regulatory elements important for supporting gene expression in calvarial osteoblasts: (i) the GCAGTCA motif of the OCFRE (*45*), (ii) the ACCACA motif (TGTGGT bottom strand) mediating Cbfa1/Osf2 recognition (*5*, *8*, *39*), and (iii) a TGACCC steroid hormone receptor motif important for regulation by cyclic AMP (*43*, *45*). This suggests that the N-terminal domain of MINT functions as a repressor of the OC promoter in cotransfection assays by regulating access of these transcriptional activators to their cognate elements. Our data indicate that MINT expression is regulated during MC3T3E1 osteoblast differentiation in culture. Future experiments will examine the interactions between MINT, Msx2, and Dlx5 to transcription factor "loading" of the proximal OC promoter during sequential elaboration of the osteoblast phenotype (*1*, *59*). Intriguingly, MINT(1−812) can also upregulate promoter activity driven by the HSV TK promoter in osteoblasts. Whether MINT directly recognizes and transactivates HSV TK promoter or functions via derepression (i.e., downregulation of an inhibitor) remains to be tested. However, our data directly demonstrate that the N-terminal domain of MINT functions as a transcription factor. As observed with other transcriptional regulators (*60*), MINT transcriptional regulatory function depends on promoter context.

The functional relationships between the N-terminal RRM containing domain and the downstream Msx2 binding domain of MINT have yet to be established. To date—despite extensive experimentation with multiple protease inhibitor cocktails and extraction protocols—we have never immunovisualized a 390 kDa protein in any cellular fraction that could represent the full-length, nascent MINT polypeptide. However, we do readily observe two separate nuclear MINT protein fragments of 110 kDa (Figure 4) and 250 kDa (Figure 5); these accumulating MINT protein fragments were individually visualized using affinity-purified antibodies raised against the extreme N-terminus and the internal Msx2 binding domain. The observation that antibodies to widely spaced domains recognize two immunologically distinct, "smaller" nuclear MINT proteins suggests that nascent MINT polypeptide is either cotranslationally or rapidly posttranslationally processed by proteolytic cleavage—somewhere between residues 1000 and 2000, severing the N-terminal RRM domain from the internal Msx2 binding domain (Figure 3). Consistent with this, the 110 kDa N-terminal MINT protein binds to an oligo(dT) affinity resin (Figure 4), and the endogenous 250 kDa MINT protein fragment binds Msx2 (Figure 5) but does not bind oligo(dT) (unpublished observations). Under nonreducing conditions, it remains possible that the two MINT protein fragments remain associated via disulfide bond formation—as occurs after nascent insulin receptor polypeptide processing (*61*). Our exhaustive attempts to perform immunoprecipitations from chromatin and nuclear matrix fractions under minimally reducing conditions have been unsuccessful due to the formation of insoluble protein aggregates that contain MINT (unpublished). Pulse−chase and confocal immunofluorescence studies (*62*) with multiple monospecific polyclonal antibodies spanning the

entire MINT protein will be necessary to characterize the cell biology of nascent MINT polypeptide processing and to detail the possible role of Msx2 in the regulation of MINT protein maturation in osteoblasts.

The RRM was initially characterized as a ca. 75 amino acid RNA binding module of proteins involved in RNA processing and transport (*54*). Each individual RRM contains two ribonucleoprotein consensus sequences that adopt a $\beta\alpha\beta\beta\alpha\beta$ secondary structure characterized by a four-stranded antiparallel β-sheet. Our observation that the MINT N-terminal RRM domain recognizes and regulates the OC promoter extends the recent discovery by Childs and coworkers (*36*, *37*) that tandem RRMs can function as authentic single-stranded and double-stranded DNA binding modules for transcription factors. In an elegant series of experiments characterizing H1β gene regulation, they identified that the sea urchin transcription factor SSAP (stage-specific activator protein) recognizes and activates a blastula-specific enhancer via an RRM-containing domain (*36*, *37*). Like the MINT RRM domain, the SSAP RRM domain binds DNA in a sequence-specific fashion and recognizes both dsDNA and ssDNA cognates. Similarly, hTAFII68, a component of TFIID, also binds nucleic acid via an RRM domain and recognizes both RNA and DNA cognates (*38*). Thus, MINT is a new member of an expanding class of novel transcriptional regulators that exhibit both ssDNA and dsDNA binding activity, conferred by RRM domains.

The identification of multiple RRM domains in MINT and SSAP suggests that the DNA binding cognates for this class of transcription factor may in fact be multipartite, with recognition encoded in the combinatorial specificity of the individual RRMs. MINT(1−546) has three individual RRMs that vary in their overall relationship to the Pfam RRM domain model, with the first RRM at 269−341 (*E*-value = 0.02) much more distantly related to the domain model than the other two RRMs at 370−446 (*E*-value = 1.7×10^{-11}) and 450−522 (*E*-value = 4.6×10^{-13}). It is intriguing to note that, in our competition studies using radiolabeled dT-20, addition of unlabeled dG-20 gave rise to a larger supershifted DNA−protein complex—indicating multimerization via a separate binding site—and only weakly inhibited binding to dT-20. In contrast, dT-20 gives rise only to monotonic competition. It is intriguing to speculate that the two arms of the imperfect OC promoter G/T-rich inverted repeat are individually recognized by a unique pair of RRMs provided by the MINT N-terminal domain. On the basis of our competition studies with dG-20 (Figure 8), we conclude that the G-residues in the duplex OC GTIR sequences are largely responsible for the stable formation of DNA−MINT-(1−546) interactions. Future structure−function studies will reveal how the cognate preferences and spacing of individual RRM domains contribute to the overall DNA binding specificity of MINT and the organizational constraints of composite cognate elements.

The only other Msx2 binding protein isolated by expression cloning, Miz1 (also known as ARIP3), has a proline-rich domain similar to the Msx2 binding domain of MINT-(2070−2394). Like Msx2 (ref *53* and our unpublished observations) and MINT (this work), Miz1/ARIP3 is highly expressed in mouse testis (*63*, *64*). Craniofacial osteoblasts and odontoblasts express both MINT and Msx2 (Figure 4 and unpublished observations); whether Miz1/ARIP3 is also expressed in the craniofacial tissues is unknown. However, since MINT is widely expressed, we surmise that MINT participates in gene regulation in multiple cell types. The full spectrum of cellular targets regulated by MINT during vertebrate development remains to be delineated.

ACKNOWLEDGMENT

We thank Emily Jackson-Machelski of the Departmental Nucleic Acid Sequencing Core Laboratory for her technical assistance.

REFERENCES

1. Bilezikian, J. P., Raisz, L. G., and Rodan, G. A. (1996) *Principles of bone biology*, Academic Press, San Diego.
2. Kim, H. J., Rice, D. P., Kettunen, P. J., and Thesleff, I. (1998) *Development 125*, 1241−1251.
3. Vainio, S., Karavanova, I., Jowett, A., and Thesleff, I. (1993) *Cell 75*, 45−58.
4. Banerjee, C., McCabe, L. R., Choi, J. Y., Hiebert, S. W., Stein, J. L., Stein, G. S., and Lian, J. B. (1997) *J. Cell. Biochem. 66*, 1−8.
5. Ducy, P., Zhang, R., Geoffroy, V., Ridall, A. L., and Karsenty, G. (1997) *Cell 89*, 747−754.
6. Komori, T., Yagi, H., Nomura, S., Yamaguchi, A., Sasaki, K., Deguchi, K., Shimizu, Y., Bronson, R. T., Gao, Y. H., Inada, M., Sato, M., Okamoto, R., Kitamura, Y., Yoshiki, S., and Kishimoto, T. (1997) *Cell 89*, 755−764.
7. Otto, F., Thornell, A. P., Crompton, T., Denzel, A., Gilmour, K. C., Rosewell, I. R., Stamp, G. W., Beddington, R. S., Mundlos, S., Olsen, B. R., Selby, P. B., and Owen, M. J. (1997) *Cell 89*, 765−771.
8. Geoffroy, V., Ducy, P., and Karsenty, G. (1995) *J. Biol. Chem. 270*, 30973−30979.
9. Sato, M., Morii, E., Komori, T., Kawahata, H., Sugimoto, M., Terai, K., Shimizu, H., Yasui, T., Ogihara, H., Yasui, N., Ochi, T., Kitamura, Y., Ito, Y., and Nomura, S. (1998) *Oncogene 17*, 1517−1525.
10. Selvamurugan, N., Chou, W. Y., Pearman, A. T., Pulumati, M. R., and Partridge, N. C. (1998) *J. Biol. Chem. 273*, 10647−10657.
11. Imhof, A., Yang, X. J., Ogryzko, V. V., Nakatani, Y., Wolffe, A. P., and Ge, H. (1997) *Curr. Biol. 7*, 689−692.
12. Hoffmann, H. M., Catron, K. M., van Wijnen, A. J., McCabe, L. R., Lian, J. B., Stein, G. S., and Stein, J. L. (1994) *Proc. Natl. Acad. Sci. U.S.A. 91*, 12887−12891.
13. Newberry, E. P., Latifi, T., Battaile, J. T., and Towler, D. A. (1997) *Biochemistry 36*, 10451−10462.
14. Newberry, E. P., Boudreaux, J. M., and Towler, D. A. (1997) *J. Biol. Chem. 272*, 29607−29613.
15. Newberry, E. P., Latifi, T., and Towler, D. A. (1998) *Biochemistry 37*, 16360−16368.
16. Satokata, I., and Maas, R. (1994) *Nat. Genet. 6*, 348−356.
17. Winograd, J., Reilly, M. P., Roe, R., Lutz, J., Laughner, E., Xu, X., Hu, L., Asakura, T., vander Kolk, C., Strandberg, J. D., and Semenza, G. L. (1997) *Hum. Mol. Genet. 6*, 369−379.
18. Towler, D. A., Rutledge, S. J., and Rodan, G. A. (1994) *Mol. Endocrinol. 8*, 1484−14893.
19. Towler, D. A., Bennett, C. D., and Rodan, G. A. (1994) *Mol. Endocrinol. 8*, 614−624.
20. Ma, L., Golden, S., Wu, L., and Maxson, R. (1996) *Hum. Mol. Genet. 5*, 1915−1920.
21. Liu, Y. H., Tang, Z., Kundu, R. K., Wu, L., Luo, W., Zhu, D., Sangiorgi, F., Snead, M. L., and Maxson, R. E. (1999) *Dev. Biol. 205*, 260−274.
22. Liu, Y. H., Kundu, R., Wu, L., Luo, W., Ignelzi, M. A., Jr., Snead, M. L., and Maxson, R. E., Jr. (1995) *Proc. Natl. Acad. Sci. U.S.A. 92*, 6137−6141.
23. Zhang, H., Hu, G., Wang, H., Sciavolino, P., Iler, N., Shen, M. M., and Abate-Shen, C. (1997) *Mol. Cell. Biol. 17*, 2920−2932.

24. Zhang, H., Catron, K. M., and Abate-Shen, C. (1996) *Proc. Natl. Acad. Sci. U.S.A. 93*, 1764−1769.
25. Woloshin, P., Song, K., Degnin, C., Killary, A. M., Goldhamer, D. J., Sassoon, D., and Thayer, M. J. (1995) *Cell 82*, 611−620.
26. Ryoo, H. M., Hoffmann, H. M., Beumer, T., Frenkel, B., Towler, D. A., Stein, G. S., Stein, J. L., van Wijnen, A. J., and Lian, J. B. (1997) *Mol. Endocrinol. 11*, 1681−1694.
27. Bidder, M., Latifi, T., and Towler, D. A. (1998) *J. Bone Miner. Res. 13*, 609−619.
28. Dodig, M., Kronenberg, M. S., Sumoy, L., Pan, Z., Upholt, W. B., Gerstenfeld, L. C., and Lichtler, A. C. (1996) *J. Bone Miner. Res. 11* (Suppl. 1), S260 (Abstract).
29. Kurokawa, R., Kalafus, D., Ogliastro, M. H., Kioussi, C., Xu, L., Torchia, J., Rosenfeld, M. G., and Glass, C. K. (1998) *Science 279*, 700−703.
30. Karin, M., Liu, Z., and Zandi, E. (1997) *Curr. Opin. Cell Biol. 9*, 240−246.
31. McInerney, E. M., Rose, D. W., Flynn, S. E., Westin, S., Mullen, T. M., Krones, A., Inostroza, J., Torchia, J., Nolte, R. T., Assa-Munt, N., Milburn, M. V., Glass, C. K., and Rosenfeld, M. G. (1998) *Genes Dev. 12*, 3357−3368.
32. Kadonaga, J. T. (1998) *Cell 92*, 307−313.
33. Korzus, E., Torchia, J., Rose, D. W., Xu, L., Kurokawa, R., McInerney, E. M., Mullen, T. M., Glass, C. K., and Rosenfeld, M. G. (1998) *Science 279*, 703−707.
34. Blanar, M. A., and Rutter, W. J. (1992) *Science 256*, 1014−1018.
35. Bateman, A., Birney, E., Durbin, R., Eddy, S. R., Finn, R. D., and Sonnhammer, E. L. (1999) *Nucleic Acids Res. 27*, 260−262.
36. DeAngelo, D. J., DeFalco, J., Rybacki, L., and Childs, G. (1995) *Mol. Cell. Biol. 15*, 1254−1264.
37. DeFalco, J., and Childs, G. (1996) *Proc. Natl. Acad. Sci. U.S.A. 93*, 5802−5807.
38. Bertolotti, A., Lutz, Y., Heard, D. J., Chambon, P., and Tora, L. (1996) *EMBO J. 15*, 5022−5031.
39. Merriman, H. L., van Wijnen, A. J., Hiebert, S., Bidwell, J. P., Fey, E., Lian, J., Stein, J., and Stein, G. S. (1995) *Biochemistry 34*, 13125−13132.
40. Schubeler, D., Mielke, C., Maass, K., and Bode, J. (1996) *Biochemistry 35*, 11160−11169.
41. Barnes, W. M. (1994) *Proc. Natl. Acad. Sci. U.S.A. 91*, 2216−2220.
42. Sambrook, J., Fritsch, E. F., and Maniatis, T. (1989) *Molecular cloning: a laboratory manual*, 2nd ed., Cold Spring Harbor Laboratory, Cold Spring Harbor, NY.
43. Towler, D. A., and Rodan, G. A. (1995) *Endocrinology 136*, 1089−1096.
44. Newberry, E. P., Willis, D., Latifi, T., Boudreaux, J. M., and Towler, D. A. (1997) *Mol. Endocrinol. 11*, 1129−1144.
45. Boudreaux, J. M., and Towler, D. A. (1996) *J. Biol. Chem. 271*, 7508−7515.
46. Harlow, E., and Lane, D. (1988) *Antibodies: a laboratory manual*, Cold Spring Harbor Laboratory, Cold Spring Harbor, NY.
47. Peterson, G. L. (1977) *Anal. Biochem 83*, 346−356.
48. Dignam, J. D., Lebovitz, R. M., and Roeder, R. G. (1983) *Nucleic Acids Res. 11*, 1475−1489.
49. Altschul, S. F., Madden, T. L., Schaffer, A. A., Zhang, J., Zhang, Z., Miller, W., and Lipman, D. J. (1997) *Nucleic Acids Res. 25*, 3389−3402.
50. Kozak, M. (1987) *Nucleic Acids Res. 15*, 8125−8148.
51. Kozak, M. (1986) *Cell 44*, 283−292.
52. Sonnhammer, E. L., Eddy, S. R., Birney, E., Bateman, A., and Durbin, R. (1998) *Nucleic Acids Res. 26*, 320−322.
53. Fey, E. G., Wan, K. M., and Penman, S. (1984) *J. Cell Biol. 98*, 1973−1984.
54. Burd, C. G., and Dreyfuss, G. (1994) *Science 265*, 615−621.
55. Mann, R. S., and Affolter, M. (1998) *Curr. Opin. Genet. Dev. 8*, 423−429.
56. Mann, R. S. (1995) *Bioessays 17*, 855−863.
57. Tan, S., and Richmond, T. J. (1998) *Nature 391*, 660−666.
58. Frenkel, B., Capparelli, C., Van Auken, M., Baran, D., Bryan, J., Stein, J. L., Stein, G. S., and Lian, J. B. (1997) *Endocrinology 138*, 2109−2116.
59. Stein, G. S., and Lian, J. B. (1993) *Endocr. Rev. 14*, 424−442.
60. Reichardt, H. M., Kaestner, K. H., Tuckermann, J., Kretz, O., Wessely, O., Bock, R., Gass, P., Schmid, W., Herrlich, P., Angel, P., and Schutz, G. (1998) *Cell 93*, 531−541.
61. Kahn, C. R., and White, M. F. (1988) *J. Clin. Invest. 82*, 1151−1156.
62. Zeng, C., McNeil, S., Pockwinse, S., Nickerson, J., Shopland, L., Lawrence, J. B., Penman, S., Hiebert, S., Lian, J. B., van Wijnen, A. J., Stein, J. L., and Stein, G. S. (1998) *Proc. Natl. Acad. Sci. U.S.A. 95*, 1585−1589.
63. Moilanen, A. M., Karvonen, U., Poukka, H., Yan, W., Toppari, J., Janne, O. A., and Palvimo, J. J. (1999) *J. Biol. Chem. 274*, 3700−3704.
64. Wu, L., Wu, H., Ma, L., Sangiorgi, F., Wu, N., Bell, J. R., Lyons, G. E., and Maxson, R. (1997) *Mech. Dev. 65*, 3−17.

BI990967J